https://doi.org/10.5194/amt-2024-110
Preprint. Discussion started: 28 June 2024

Atmospheric Measurement Techniques Discussions

EMADDC: high quality, quickly available and high volume wind and temperature observations from aircraft using the Mode-S EHS infrastructure

Siebren de Haan[1], Paul de Jong[1,*], Michal Koutek[1,*], and Jan Sondij[1]

[1]KNMI, PO 201, 3730 AE De Bilt
[*]These authors contributed equally to this work.

Correspondence: Siebren de Haan (Siebren.de.Haan@knmi.nl)

Abstract. Temperature and wind observations from aircraft are regarded of major importance for aviation meteorology and numerical weather prediction (NWP). The European Meteorological Aircraft Derived Data Center (EMADDC) system processes aircraft surveillance data received from air traffic control (ATC) and converts it into observations of wind and temperature. Only so-called Mode-S Enhanced Surveillance data can be used, because this data contains the air vector and ground vector of the aircraft, from which a wind vector can be inferred. To acquire high quality observations, the data is processed in three steps: pre-processing, processing, and post-processing. The pre-processing is needed to obtain high-quality information and to calculate several correction values such as temperature corrections and heading corrections. Processing converts the aircraft data into meteorological information and finally post-processing guarantees that only high-quality information is made available. The quality of the observations produced is verified by comparing these observation to other upper air wind and temperature observations from radiosondes and comparing them with NWP data. This paper presents the EMADDC system, operational since 2019.

1 Introduction

For normal, and safe, operation, aircraft are equipped with sensors to measure for example its height, and velocity with respect to the surrounding air. These sensors can be exploited to observe wind and temperature at the aircraft's location (Painting, 2003). For many years, aircraft observations form the backbone of the global observing system which is used as input for numerical weather prediction models during assimilation (Cardinali et al., 2003; James et al., 2020; Li, 2021; Strajnar et al., 2015; de Haan, 2013). For almost 30 years, aircraft measurements have been collected using the Aircraft Meteorological Data Relay (AMDAR), where meteorological information is automatically sent to national weather services using either satellites or ground stations (Ingleby et al., 01/2020 2020; Barwell and Lorenc, 1985; Cardinali et al., 2003; James et al., 2020; Lange and Janjić, 2016; Li, 2021; Petersen, 2016; Zhu et al., 2015; Benjamin et al., 2010). Dedicated aircraft were equipped with software to collect the relevant information from the onboard computer systems. Observations are collected with specified observation strategies to optimize coverage with respect to data transmission costs. The last decade, a different manner of collecting meteorological information was developed utilizing the operational infrastructure for aircraft safety in Europe, starting in the

https://doi.org/10.5194/amt-2024-110
Preprint. Discussion started: 28 June 2024


Atmospheric Measurement Techniques Discussions

area of Germany, Belgium and The Netherlands. The infrastructure used by the European Air Traffic Control (ATC) is based on Mode-selective (Mode-S) radars which (selectively) interrogate all aircraft in view of the radar on information on the intended heading, airspeed etc., to guide aircraft through its airspace (de Haan, 2011). Although in the whole European airspace Mode-S radars are used for ATC, not all received information can be used to refer to meteorological information, only Mode-S enhanced surveillance (Mode-S EHS) radars can interrogate the necessary BDS5.0 and BDS6.0 registers. Fortunately, the most of Mode-S radars in Europe have EHS capabilities. The observation frequency is determined by the interrogation frequency of the Mode-S radar. To extract meteorological information from the received BDS5.0 and BDS6.0 registers, processing and corrections are needed (de Haan, 2011). Due to the COVID19-pandemic, the number of flights dramatically decreased (Dube, 2023) and with it the availability of temperature and wind observations performed by dedicated aircraft collected through Aircraft Meteorological Data Relay (AMDAR). However, whilst some airlines were still flying (e.g. cargo flights), the European Meteorological Aircraft Derived Data Center (EMADDC) was still producing valuable observations, exploiting the ATC information received for surveillance. These observations were used by ECMWF-IFS (Ingleby et al., 2021).

This paper describes the current state of the art implemented processing and correction methodology as implemented for the EMADDC.

2 EMADDC Data Collection

Secondary Surveillance Radar (SSR) is a two-way system where an ATC radar interrogates an aircraft requesting specific parameters. In Europe, all large aircraft (with so-called minimum take-off weight larger than 5700 kg) are required to broadcast Mode-S Elementary Surveillance (ELS) and Enhanced Surveillance (EHS) (1207, 2011). The EMADDC processing system derives wind speed, wind direction and temperature observations from surveillance data requested from aircraft for ATC purposes. Where Elementary Surveillance only broadcasts altitude and identity, Enhanced Surveillance complements these basic parameters with data of the aircraft state, such as roll angle, air speed and Mach number. These additional parameters are requested in groups as a BDS request. To derive wind and temperature, EMADDC requires both BDS5.0 and BDS6.0 to be interrogated.

Additional to these mandatory BDS registers, BDS4.4, known as the Meteorological Routine Air Report or MRAR can be also interrogated, which will request the observed temperature, wind, static pressure and humidity. However, this register is not mandatory and only few (less than 5%) aircraft respond to such interrogation requests (Strajnar, 2012). This is also the reason only few countries actively interrogate this register to reduce over-interrogation.

2.1 Mode-S EHS Interrogation

ATC radar sends an interrogation or request to an aircraft requesting a response for certain BDS registers. The aircraft in turn will respond, if it is equipped, and broadcasts the requested register. It should be noted that not all Mode-S equipped radars are able to interrogate all the required registers to derive temperature and wind or do not interrogate all BDS registers during each radar rotation. Each country or Air Traffic Service Air Navigation Service Provider (ATS ANSP) may interrogate aircraft

https://doi.org/10.5194/amt-2024-110
Preprint. Discussion started: 28 June 2024

Atmospheric Measurement Techniques Discussions

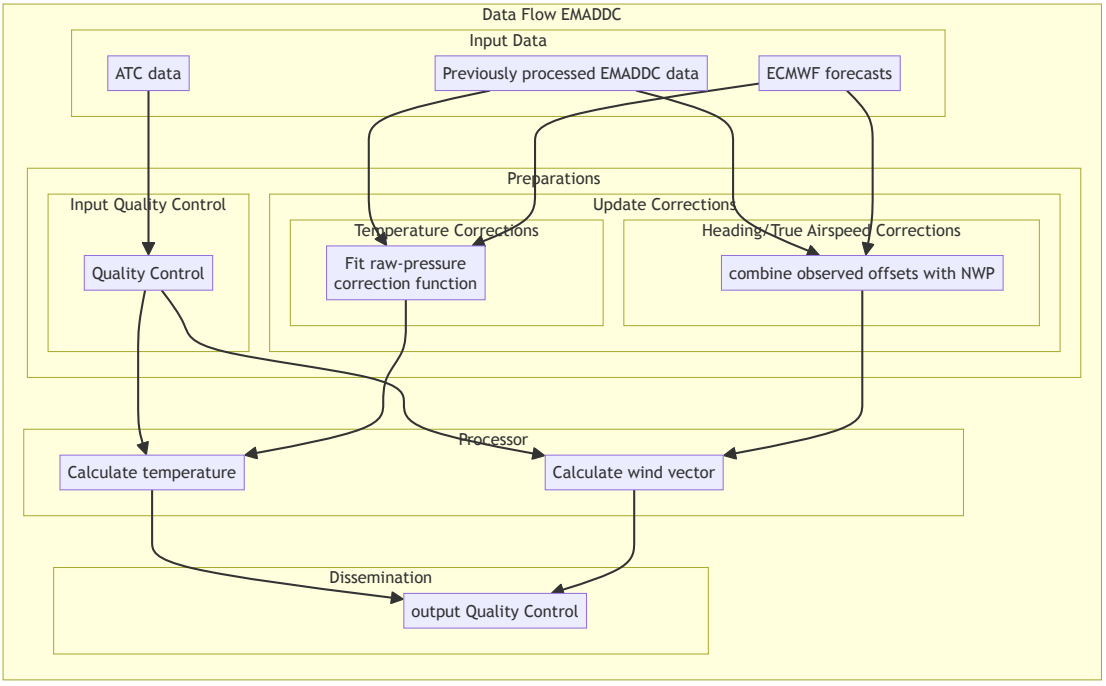

Figure 1. Functional data flow in EMADDC, needed to derive wind vector and temperature observations.

differently and at various times and rates. The response sent by the aircraft is received by ATC radar but can also be received through a commercially available local Mode-S/ADS-B receiver, as data is not encrypted. Unfortunately, it is more difficult to decode data received by these reseceivers as the type of register is not contained in the transmission and hence fuzzy logic or other techniques shall be applied to decode the type transmitted properly.

2.2 Aircraft Dependent Surveillance-Broadcast

Aircraft Dependent Surveillance-Broadcast, or ADS-B, as its name suggests, allows an aircraft to broadcast aircraft state data using the transponder. Data is autonomously broadcast about every 0.5 seconds and contains the aircraft's onboard sensed position (through GPS and inertial systems) which is often more accurate than radar derived position from ATC. This data is available to ATC but also displayed on the Navigation Display of newer aircraft for situational awareness. ADS-B does not broadcast wind and temperature, nor does it broadcast all required parameters to derive wind and temperature, allthough the difference between GNSS height and pressure altitude is transmitted frequently and could be used in data assimilation (**?**). Note that the content of messages is may differ for each aircraft.

https://doi.org/10.5194/amt-2024-110
Preprint. Discussion started: 28 June 2024


Atmospheric Measurement Techniques Discussions

2.3 Aircraft Dependent Surveillance-Contract

Aircraft Dependent Surveillance-Contract (ADS-C) differs from ADS-B as it reports to a single ground station in control of the contract. The ground station controls the content of the data to be transmitted back. The content can contain observed wind and temperature and even the aircraft trajectory. The update rate is typically lower than that of ADS-B.

3 Data Handling

EMADDC receives aircraft data directly from ATC, or by collection using a local Mode-S/ADS-B receiver. The first method delivers data of high quality as the content is properly decoded since the content of each transmission is known. ATC also supplies quality control and filtering on the data supplied. Data can be of ASTERIX CAT48 format, which is mono-radar data or CAT62 data from a radar tracker. This latter data uses filtering to sample all radar plots to a typical 4 second interval. The content of these formats is similar but the typical resolution of the Mach number in CAT62 is lower and hence the derived temperature are of lower quality. For this, multiple solutions are available where the first uses a different parameter field to supply the Mach number in higher resolution. EMADDC is working with EUROCONTROL MUAC to develop a solution. Another option is to derive the Mach number from the indicated airspeed (Straus, 2020). An advantage of radar or tracker data is that BDS messages are combined into a single "observation" message. For radar or tracker data, the position is determined by ATC radar while for data received by a local receiver, the position is decoded from the Compact Position Report (CPR) format which is part of the ADS-B message, and the timestamp is supplied by the receiver and not by the aircraft and EMADDC-system needs to combine the different BDS-registers to derive observations.

The techniques applied by EMADDC are delivering enormous amounts of high-quality data from Mode-S EHS data. However, several quality control checks need to be applied to capture observation imperfections.

4 Aircraft measurement methodology

A modern aircraft is equipped with sensors that can measure static pressure or pressure altitude, Mach number, temperature, position and heading, and Geometric altitude. This section conains a brief description of measurements of pressure, Mach and temperature.

4.1 Mach number and static and total pressure

The pitot-tube measures the static pressure p_s and the total pressure p_t (Ruijgrok, 1990). Both pressure observations suffer from inaccuracies related to for example a (small) angle between the flow and the probe (Rodi and Leon, 2012). The Mach number is the airspeed of the aircraft relative to the speed of sound. It is measured (almost directly) by a pitot-probe. Let $q_t = p_t - p_s$ be the dynamic pressure, which is more accurately measured because the first order error of p_t and p_s are canceled. Then

$$M = \sqrt{5\left(1 + \frac{q_t}{p_s}\right)^{2/7} - 1} \tag{1}$$

https://doi.org/10.5194/amt-2024-110
Preprint. Discussion started: 28 June 2024

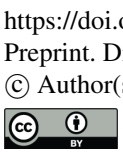

Atmospheric Measurement Techniques Discussions

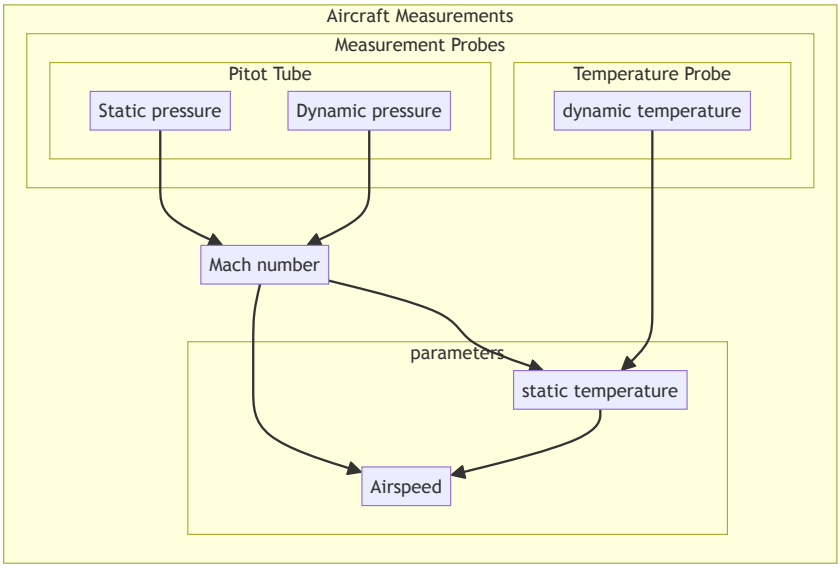

Figure 2. Information flow of aircraft measurements

Note that the dependence of M on the (inaccurate) p_s remains.

4.2 Temperature

The temperature is measured with a temperature probe (Ruijgrok, 1990). The measured total temperature T_t needs to be corrected to obtain the (ambient) temperature T,

$$T_t = T\left(1 + \lambda \frac{(\gamma - 1)}{2} M^2\right) \tag{2}$$

5 EMADDC Measurement Methodology

5.1 Downlinked parameters

The (most relevant) parameters obtained through interrogation of Mode-S EHS radars are shown in Table 1. The timestamp is created at the moment of arrival of the information. All parameters that originate from interrogation, have an observation frequency depending on the radar, however ADS-B information can have an observation frequency of twice per second. Table 1 displays some information of the downlinked parameters. The information flow of the downlinked parameters is depicted in Figure 3. Also shown in this figure are the corrections applied to the magnetic heading, airspeed and Mach-number, discussed later.

https://doi.org/10.5194/amt-2024-110
Preprint. Discussion started: 28 June 2024

Atmospheric Measurement Techniques Discussions

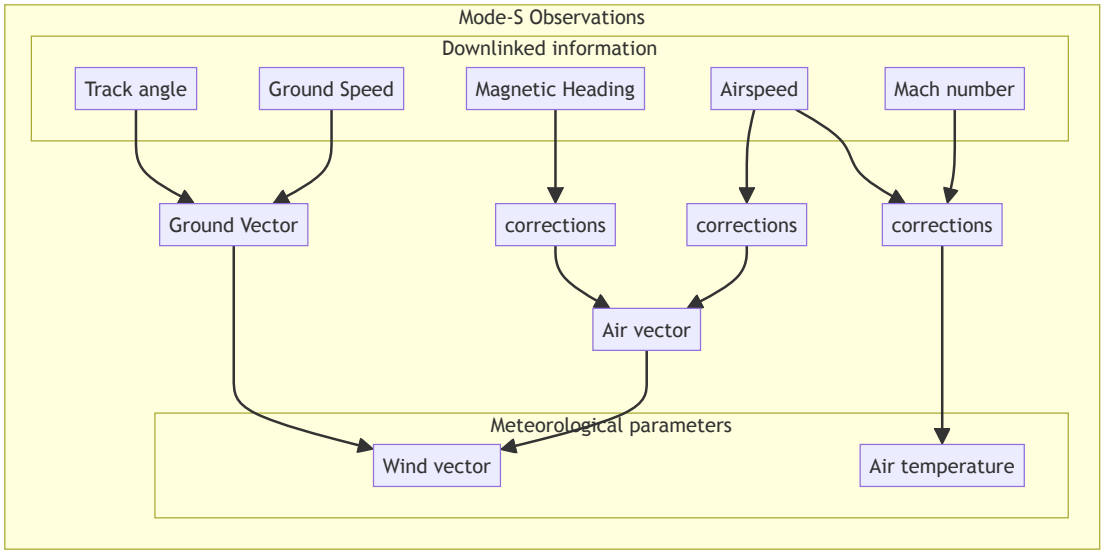

Figure 3. Downlinked data flow of Mode-S EHS observations to acquire meteorological information.

5.2 Raw data input control

The EMADDC quality procedure has been developed and refined in the last decade. The first step in defining the quality is to check the input for obvious errors, as listed in Table 2. Measurements fulfilling one of these checks are discarded from further processing.

5.3 Output control and whitelisting

Output control is necessary to obtain good quality observations. The parameters for output quality control are related to the corrections methods applied to the temperature and wind measurement. Additionally, whitelisting is performed to ensure that observations are within three times standard deviation of the measurement with NWP model equivalents. EMADDC currently uses the operational ECMWF IFS model for this comparison.

6 Derived temperature

Although the temperature is measured by the sensors onboard the aircraft, the information is not transmitted in the Mode-S EHS request BDS5.0 and BDS6.0. However, the Mach number M and the airspeed A are available and from these paramters the temperature can be deduced using the relation between the speed of sound and temperature and the ideal gas law,

$$M = \frac{A}{C}, \tag{3}$$

https://doi.org/10.5194/amt-2024-110
Preprint. Discussion started: 28 June 2024

Atmospheric Measurement Techniques Discussions

Table 1. The reported accuracy and observation frequency of downlinked parameters.

parameter	abbreviation	symbol	frequency	reported accuracy	unit	BDS
Position (latitude/longitude)	lat,lon	λ, ϕ		0.5s - 2s		ADS-B / Track
Flight Level	fl		0.25	5s - 20s	100 ft	ADS-B
Roll Angle	ra		0.175	5s - 20s	degrees	5.0
True Track Angle	tta	t	0.175	5s - 20s	degrees	5.0
Groundspeed	gspd	G	2	5s - 20s	knots	5.0
Track Angle Rate	tar		0.03125	5s - 20s	degrees/sec	5.0
True Airspeed	tas	A	2	5s - 20s	knots	5.0
Magnetic Heading	mhdg	h_m	0.352	5s - 20s	degrees	6.0
Indicated Airspeed	ias	A^I	1	5s - 20s	knots	6.0
Mach Number	mach	M	0.004	5s - 20s	-	6.0
Barometric Altitude Rate	bar		32	5s - 20s	ft/min	6.0
Inertial Vertical Velocity	ivv		32	5s - 20s	ft/min	6.0
East-West Velocity	gspd-u	G_u	1	0.5s - 2s	knots	0.9 (subtype 1)
North-South Velocity	gspd-v	G_v	1	0.5s - 2s	knots	0.9 (subtype 1)
Vertical Rate			64	0.5s - 2s	ft/min	0.9 (subtype 1,2)
GNSS height offset			25	0.5s - 2s	ft	0.9 (subtype 1,2)
Magnetic Heading	mhdg	h_m	0.352	0.5s - 2s	degrees	0.9 (subtype 3,4)
True Airspeed	tas	A	1	0.5s - 2s	knots	0.9 (subtype 3)
Vertical Rate			64	0.5s - 2s	ft/min	0.9 (subtype 3,4)
Geometric height offset			25	0.5s - 2s	ft	0.9 (subtype 3,4)

Table 2. Current input quality checks used in operation.

	Input data quality checks
1	absolute value of roll angle larger than 2.5 degrees,
2	absolute difference between track angle and magnetic heading larger than 25 degrees
4	true air speed larger than 570 kts or smaller than 100 kts
5	groundspeed larger than 850 kts or smaller than 50 kts, or when below flight level 50 smaller than 100kts
6	Mach number smaller than 0.001
7	constant flight level and decreasing ground speed and indicated airspeed when fl is lower than 50
8	flightlevel lower than -100

https://doi.org/10.5194/amt-2024-110
Preprint. Discussion started: 28 June 2024


Atmospheric Measurement Techniques Discussions

where $C = \sqrt{\gamma R_d T}$, where $\gamma = c_p/c_v$ is the ratio of specific heats and R_d is the universal gas constant for dry air. Thus, given M and A, the temperature T can be calculated by

$$T = \frac{1}{\gamma R_d}\left(\frac{A}{M}\right)^2, \tag{4}$$

where A is in [m/s].

6.1 Temperature measurement improvements

The aircraft measurements are improved by algorithms onboard the aircraft. The applied corrections are not available and may be aircraft dependent, or aircraft type dependent, or both. It is known that the measurement of the static pressure p_s suffers from airflow instabilities and/or angle of attack (Rodi and Leon, 2012). The static pressure is corrected, which consequently results in a correction of the Mach number M and temperature T.

6.2 Aircraft dependent temperature bias correction

A temperature correction is constructed using auxiliary temperature information, obtained from NWP. The temperature measurement depends on the Mach number, which in turn depends on pressure, and pressure, at low altitude, is less accurate. Therefore, an improved pressure value that would result in a measurement of temperature T, given the dynamic pressure q_t and true airspeed A. To accommodate this, for each aircraft these corrected values of pressure are stored and used to determine a relation between the corrected pressure, the original pressure and the true airspeed. In this a corrected temperature is obtained by recalculating the temperature with corrected pressure information, derived from the fit of the corrected pressure values by function p_{cor}. This function, which depends on pressure and true airspeed, is defined as

$$p_{cor} = a + bp_s + c\frac{p_s}{A^2} \tag{5}$$

where the coefficients a, b and c are found by fitting and are aircraft dependent. The procedure used is described in more detail in de Haan et al. (2022)

7 Derived wind measurement

The wind vector is the difference between ground vector and air vector, where all vectors are with respect to true North.

$$V\begin{pmatrix}\cos(d)\\ \sin(d)\end{pmatrix} = G\begin{pmatrix}\cos(t)\\ \sin(t)\end{pmatrix} - A\begin{pmatrix}\cos(h)\\ \sin(h)\end{pmatrix} \tag{6}$$

The heading is reported with respect to the magnetic North Pole and needs to be converted into a heading with respect to true North. For this purpose, geomagnetic declination tables from (Maus and Macmillan, 2005; Chulliat, 2015) are applied, thus

$$h = h_m + \delta(y, \lambda, \phi), \tag{7}$$

https://doi.org/10.5194/amt-2024-110
Preprint. Discussion started: 28 June 2024

Atmospheric Measurement Techniques Discussions

where y is the the datum, and, (λ, ϕ) is the location of the aircraft and δ is the applied heading correction. As it turns out, the heading correction is aircraft dependent, that is y is aircraft dependent, and even may change in time after an aircraft is being serviced, for example when the computer software is updated.

7.1 Aircraft dependent heading correction

Although the correction should be in the order of the (actual) declination, previous research found that a simple correction is not enough (de Haan, 2011). As it turns out, each aircraft may use its own version of a declination lookup table, which implies that each aircraft corrects the true North to magnetic North in a different way. Hence, the correction method uses the assumption that the correction is determined by a geomagnetic reference table for a certain datum (or epoch) and is static until updated through aircraft maintenance. The optimal datum is found by minimizing a cost function, depending on datum, by comparing corrected winds from observations with NWP model forecast winds. The cost function is constructed by the vector length difference between the unit heading vector from the aircraft and the unit heading vector formed by the ground vector and NWP-wind vector, that is

$$\delta^i(y) = \begin{pmatrix} \cos\left(h_N^i\right) - \cos\left(h_m^i + h_c\big(y(\lambda^i, \phi^i)\big)\right) \\ \sin\left(h_N^i\right) - \sin\left(h_m^i + h_c\big(y(\lambda^i, \phi^i)\big)\right) \end{pmatrix}, \tag{8}$$

with

$$h_N^i = \operatorname{atan}\left(\frac{G^i \sin\left(t^i\right) - V^i \sin\left(d^i\right)}{G^i \cos\left(t^i\right) - V^i \cos\left(d^i\right)}\right), \tag{9}$$

and i the index of an observation, h_m^i is the observed magnetic heading and $h_c(y(\lambda^i, \phi^i))$ the value of the declination table with datum y at location (λ^i, ϕ^i). The cost function is defined as the sum of all vector length differences over all observations, that is

$$\begin{aligned} C(y) &= \frac{1}{2}\sum_i ||\delta^i(y)||^2 && (10) \\ &= \frac{1}{2}\sum_i \left(\sin\left(h_N^i\right) - \sin\left(h_m^i + h_c^i(y)\right)\right)^2 + \left(\cos\left(h_N^i\right) - \cos\left(h_m^i + h_c^i(y)\right)\right)^2 && (11) \\ &= \sum_i 1 - \cos\left(-h_N^i + h_m^i + h_c^i(y)\right) && (12) \end{aligned}$$

Next, magnetic declination is linearized with datum, that is

$$h_c^i = H_0^i + (y - y_{ref})\Delta H^i, \tag{13}$$

where H_0^i is the value of magnetic declination for given lat/lon on datum y_{ref}, ΔH^i value of the change in magnetic declination per year (this approximation is valid, as is discussed in Appendix A). We approximate the cost function by a quadratic function in the datum offset, which yields

$$C(y) \approx \sum_i \frac{\left(\Delta H^i\right)^2 \delta_y^2 \cos\left(H_0^i - h_N^i + h_m^i\right)}{2} + \Delta H^i \delta_y \sin\left(H_0^i - h_N^i + h_m^i\right) - \cos\left(H_0^i - h_N^i + h_m^i\right) + 1 \tag{14}$$

https://doi.org/10.5194/amt-2024-110
Preprint. Discussion started: 28 June 2024


Atmospheric Measurement Techniques Discussions

where

$$\delta_y = y - y_{ref} \tag{15}$$

The (offset) datum value for which the cost function attains a minimum is found by setting the derivative of the cost function to zero. Let x_1^i and x_2^i for observation i be defined by

$$x_1^i = -\Delta H^i \sin\left(H_0^i - h_N^i + h_m^i\right) \tag{16}$$

$$x_2^i = \left(\Delta H^i\right)^2 \cos\left(H_0^i - h_N^i + h_m^i\right), \tag{17}$$

then the datum minimizing the cost function is given by

$$y = y_{ref} + \frac{\sum_i x_1^i}{\sum_i x_2^i} \tag{18}$$

Using the found datum for an aircraft, EMADDC calculates the magnetic declination at the location of an observation to find the declination and converts the reported magnetic heading to true heading and calculate the wind according to the equation above.

7.2 Dependence on NWP wind vector information

The magnetic heading is calibrated using NWP wind vector information. Consequently, the obtained correction depends on the quality of the NWP information. The magnitude of this dependence is small, and of the order of one over the ground speed. Suppose we have a biased NWP wind direction, that is the true wind direction d is biased by β, then

$$\tilde{h}_N = \operatorname{atan}\left(\frac{G\sin(t) - V\sin(d+\beta)}{G\cos(t) - V\cos(d+\beta)}\right) \approx h_N + \frac{V\beta(-G\cos(d-t)+V)}{G^2 - 2GV\cos(d-t) + V^2}, \tag{19}$$

which implies that

$$|\tilde{h}_N - h_N| \lessapprox \left|\beta\frac{V(V+G)}{(G-V)^2}\right| \lessapprox \frac{|\beta|}{G} \ll |\beta|. \tag{20}$$

The offset from the true heading using wnd direction biased information is substantially smaller then the actual bias. Similarly the offset from the true heading based on wind speed biased (by α) is given by

$$|\tilde{h}_N - h_N| \lessapprox \left|\alpha\frac{G\sin(d-t))}{G^2 - 2GV\cos(d-t) + V^2}\right| \lessapprox \frac{|\alpha|}{G} \ll |\alpha|. \tag{21}$$

Since the heading correction is based on many of observations, over a large period (minimal 15 days) it can be regarded as independent of the NWP information.

7.3 True airspeed correction

The measurement of true airspeed depends on the temperature and Mach number, see equation (4). Since the observed Mach number is corrected (Rodi and Leon, 2012), the true airspeed observation can be improved likewise. The EMADDC system currently applies a true airspeed bias correction depending on aircraft and phase of flight. Future research is foreseen to come to a physical method of airspeed correction.

https://doi.org/10.5194/amt-2024-110
Preprint. Discussion started: 28 June 2024

Atmospheric Measurement Techniques Discussions

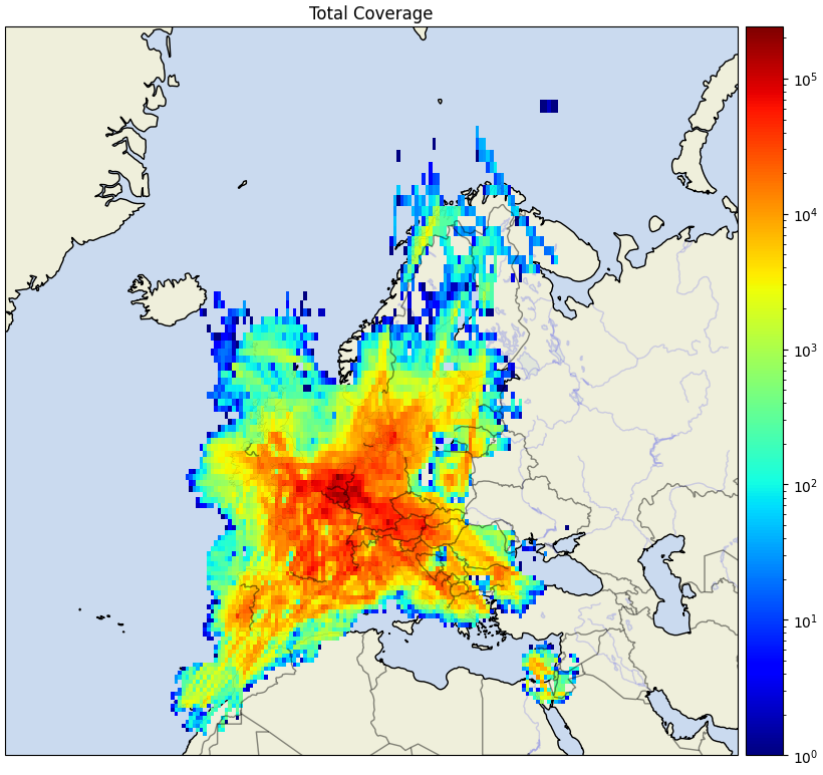

Figure 4. Data coverage of Mode-S EHS observatons on April 21st 2024. The color indicates the number of observations per 0.5 degrees squared box.

8 Processing Infrastructure

EMADDC suppliers currently provide data in 5-to-15-minute batches where the system picks up new files for ingesting into the EMADDC database. For receiver data, the data is handled by the decoder and combined to create observations from the BDS5.0 and BDS6.0 registers received and insert these into the EMADDC database. Once data is ingested into an hourly table, the processing scheduling system schedules three jobs. One processing job that contains observations of a 15 minute time window with a delay of approximately 30 minutes. In 2022, two new processing jobs that process 5-minute batches at 13 and 23-minutes past the first observation in a time window have been added to the system. These “fast” files provide about 70% and 90% of all data that is available in the regular and existing 15-minute interval files. A processing job starts by gathering all data available in the time window of interest. The input data is quality controlled, as discussed before. The last 5 minutes of the previous time window is prepended for continuation of flight profiles and phase determination. The flight profile and flight phase are used when applying the corrections. Wind and temperature are derived using equations for wind speed and wind

https://doi.org/10.5194/amt-2024-110
Preprint. Discussion started: 28 June 2024


Atmospheric Measurement Techniques Discussions

direction (see above), the detected magnetic table datum is used in the World Magnetic Model (Chulliat, 2015) to determine the magnetic declination at the location of the observation and obtain the true heading. The other corrections and post-processing is subsequently applied after which outliers are detected using a 30 seconds rolling window and median and 3 standard deviation outlier detection.

EMADDC currently receives data from overlapping sources. For example, for the EUROCONTROL MUAC area, EMADDC receive radar data from MUAC but also receiver data from 8 receivers from AirSupport. KNMI has a receiver at de Bilt and one at Cabauw at 180m receiving data up to Paris. Since technically these receivers receive the same data as the radars at ATC, EMADDC has duplicity in its database. Therefore a duplicate detection algorithm is applied where data from the same aircraft within 1 second of another observation is marked as duplicate of the primary observation. Note, that observation retrieved from Air Traffic Control directly (radar or tracker data) is never marked as a duplicate observation as ATC system apply filtering and quality control on their end and remove duplicates. Hence, it can occur that an observation is present in a fast file, but later is no longer available in the subsequent (23-minute) fast file or full time-window file as it was marked duplicate and replaced by another observation. The last processing step is to check whether observations are from aircraft that have been whitelisted. Whitelisting is performed for wind speed and temperature separately and is based on observations minus forecast statistics. Aircraft for which the 14-day standard deviation exceeds 4 kts are blacklisted while for temperature the standard deviation limit is set at 1.23 K. Finally, all valid and quality checked data is outputted in ASCII, NETCDF and BUFR files and is made available using KNMI data platform[1].

9 Results

Produced observations are continuously validated against the model and radiosondes. The tables below show the numerical weather prediction statistics over three months (January - March 2024) and radiosondes (January - March 2023).

9.1 Model comparison

In three months, a total 4.5 of billion observation were collected by the EMADDC system. From these observations 2.8 billion unique and whitelisted wind observations are made available to the users, and in total nearly 1,8 billion temperature observations are disseminated in three months. The quality of wind observations compared to ECMWF-IFS is around 2.5 [m/s] in standard deviation, with a small bias of 0.3 [m/s], see table 3. Table 3 also shows the statistics of wind and temperature observations for different height levels: the error in wind speed with respect to the model increases with height from 2.2 [m/s] near surface to 2.8 [m/s] at a height of 11 km. The wind direction statistics show a different signal; near the surface the wind direction error is nearly 15 degrees, with a minimum at around flight level 350 and increasing again to an error of 10 degrees at around 11 km. Wind is in general more variable near the surface.

[1]Please visit https://dataplatform.knmi.nl/dataset/access/emaddc-hist-repro-data-1-0

https://doi.org/10.5194/amt-2024-110
Preprint. Discussion started: 28 June 2024

Atmospheric Measurement Techniques Discussions

Table 3. Statistics of EMADDC wind observations against the operational ECMWF model

January 1, 2024 to April,1 2024

		wind speed			wind direction		
	raw volume	number	bias	std.dev	number	bias	std.dev
all data	4 546 047 080	4 384 070 442	0.34	4.76	4 281 120 981	0.14	9.62
whitelisted and unique	-	2 868 355 459	0.30	2.52	2 800 011 753	0.17	8.67
flight level	raw volume	number	bias	std.dev	number	bias	std.dev
0-100	235 608 797	151 947 715	0.20	2.20	135 707 126	-0.16	14.24
100-200	361 851 780	252 516 206	0.22	2.28	243 224 271	0.45	10.77
200-300	594 829 968	386 369 304	0.27	2.53	378 271 790	0.33	9.32
300-400	3 133 630 884	2 016 820 254	0.32	2.60	1 983 182 045	0.12	7.94
>400	220 023 701	131 427 728	0.36	2.81	128 500 903	0.02	10.03

Table 4. Statistics of EMADDC temperature observations against the operational ECMWF model

January 2024 - March 2024

		temperature		
	raw input temperature	number	bias	std.dev
all data	4 546 047 080	3 138 758 482	0.02	1.05
whitelisted and unique	-	1 763 880 586	-0.00	0.95
flight level	raw volume	bias	std.dev	
0-100	235 608 797	51 837 791	0.13	1.08
100-200	361 851 780	140 307 524	0.05	0.83
200-300	594 829 968	241 388 676	0.06	0.77
300-400	3 133 630 884	1 309 098 407	-0.01	1.04
>400	220 023 701	83 204 202	0.05	1.24

The temperature statistics are shown in Table 4. The temperature error in total is slightly smaller than 1 [K], with a minimum of error of 0.8 [K] around flight level 250. The maximum error is found at cruising level (11 km). Note that the bias with the model is around to zero.

9.2 Comparison with Radiosondes observations

Radiosondes are regarded as the anchor observation for meteorology and are generally launched at the main synoptic hours 00 UTC and 12 UTC, with some sites launching also at 06 UTC and 18 UTC. Due to budget optimization, the number of launches per day was decreased to one or two. Aircraft observations are regarded as replacement to collect upper air observations of wind and temperature. The table below shows collated observations statistics. Aircraft and observations will never be collocated in

https://doi.org/10.5194/amt-2024-110
Preprint. Discussion started: 28 June 2024

Atmospheric Measurement Techniques Discussions

Table 5. Comparison against Radiosondes

Jan 2023 - March 2023							
East-West wind component [m/s]							
		EHS - RS		EHS - NWP		RS - NWP	
flight level	number	bias	std.dev	bias	std.dev	bias	std.dev
< 50	160 746	-0.11	2.75	0.24	2.79	0.19	2.72
50 < 150	434 029	-0.09	2.13	0.17	2.40	0.23	2.24
150 < 250	565 086	-0.12	2.16	0.10	2.42	0.14	2.28
250 < 350	858 477	-0.08	2.21	0.03	2.62	0.09	2.47
350 < 450	590 015	-0.04	2.45	0.04	2.65	0.07	2.51
450 <	236	-1.55	2.42	0.81	1.98	3.08	3.56
North-South wind component [m/s]							
< 50	160 746	0.02	2.38	-0.06	2.47	-0.25	2.34
50 < 150	434 029	0.02	2.12	0.00	2.31	-0.09	2.16
150 < 250	565 086	0.02	2.27	-0.17	2.44	-0.22	2.40
250 < 350	858 477	0.01	2.33	-0.25	2.71	-0.23	2.56
350 < 450	590 015	-0.13	2.51	-0.32	2.78	-0.18	2.68
450 <	236	0.03	1.92	-0.19	2.02	-0.17	1.76
wind speed [m/s]							
< 50	160 746	-0.03	2.82	0.39	2.74	0.39	2.65
50 < 150	434 029	-0.09	2.13	0.43	2.37	0.53	2.20
150 < 250	565 086	-0.21	2.27	0.44	2.44	0.58	2.35
250 < 350	858 477	-0.07	2.37	0.45	2.74	0.49	2.59
350 < 450	590 015	0.19	2.54	0.62	2.80	0.42	2.67
450 <	236	-1.53	2.55	0.87	1.91	3.10	3.47

both space and time, moreover aircraft are warned when a nearby meteorological station launches a balloon, and avoids the balloon. Nevertheless, collocations can be made by having the maximum distance between aircraft and radiosondes of at most of 50 km and maximum height difference of 100 m and time difference of 1800 seconds. The table below shows the statistics of wind (wind speed, and the wind components) and temperature.

For all wind parameters, the comparison between radiosonde and Mode-S EHS show to have a standard deviation lower than that of the comparison is model and Mode-S EHS or radiosonde. Furthermore, the difference between model and radiosonde or model and Mode-S EHS are similar of the order of 0.3 to 0.5 m/s, while the mean difference between aircraft and balloon is small. The temperature statistics show that all three systems have the same main temperature (all biases are small and near zero). Not surprisingly, the temperature observations of Mode-S EHS are clearly of less quality than radio soundings, although above 858 hPa the quality is reasonable.

https://doi.org/10.5194/amt-2024-110
Preprint. Discussion started: 28 June 2024


Atmospheric Measurement Techniques Discussions

Table 6. Comparison against Radiosondes

Jan 2023 - March 2023							
Temperature [K]							
< 50	11 635	0.00	1.45	-0.01	1.54	-0.05	1.19
50 < 150	76 334	0.06	0.96	-0.01	0.97	-0.11	0.77
150 < 250	71 541	0.07	0.80	0.01	0.78	-0.05	0.57
250 < 350	111 700	-0.00	0.89	-0.01	0.90	0.01	0.71
350 < 450	129 903	0.05	1.14	-0.04	1.10	-0.10	1.02
450 <	23	-0.32	1.13	-0.77	1.03	-0.38	0.70

10 Conclusions

This paper presents the EMADDC system to produce wind and temperature observations derived from Mode-S EHS aircraft observations. Mode-S EHS is a surveillance method which not only tracks an aircraft in the range of the radar. It also contacts the aircraft and request special information which is used by surveillance. This downlinked data contains sufficient information to derive wind and temperature at very high spatial and temporal resolution. To be able to generate observations of good quality, several corrections and quality checks are applied. One of the important corrections is the correction from magnetic heading to true heading; this heading correction is unique for each aircraft individually.

As a reference, the wind forecast of ECMWF IFS model is used. The derived wind observations are of good quality compared to the model forecast. Note that, although the data is corrected using ECMWF forecast, the data is independent because a forecast lead time of minimal 9 hours is used, so that observation from Mode-S EHS are not used as input for assimilation and correction simultaneously.

The temperature correction is based on the methodology developed in de Haan et al. (2022). As a reference temperature again the ECMWF IFS model is used. Comparison with radiosonde observations showed good quality with respect to temperature when the obervation is above 850hPa.

Data availability. The processed data is available through the KNMI Data Platform https://dataplatform.knmi.nl.

https://doi.org/10.5194/amt-2024-110
Preprint. Discussion started: 28 June 2024

Atmospheric Measurement Techniques Discussions

Appendix A: Geomagnetic data

The datum 2015/1/1 was set as the reference datum for the declination table in the current processing setup (version 2.2 August 2023). The Geomagnetic model is used in determining the declination for a given position and time (Maus and Macmillan, 2005). Figure A1 shows the value of the declination on 2015/1/1 (left panel), the middle panel shows the yearly change in declination, and the right panel shows the difference between declination valid for 2020/1/1 and the linear approximation. The values of magnetic declination in central Europe are small. The change in declination is strongest for high latitude regions and close to zero for low latitude regions (middle panel). The error made by the linear approximation is small, as can be seen from the right panel.

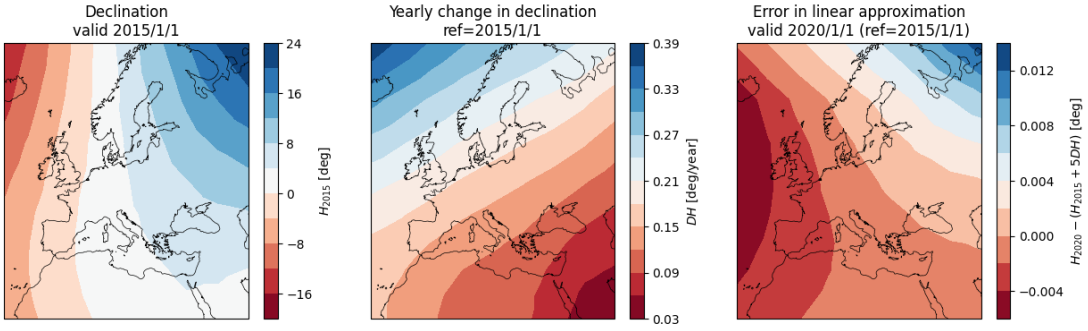

Figure A1. The effect of linearization of the declination around the datum 2015. Left panel the declination at 1st Jan. 2015; middle panel the yearly change on 1st Jan. 2015; right panel the difference between linearization and the WMM declination on 1st Jan. 2020.

https://doi.org/10.5194/amt-2024-110
Preprint. Discussion started: 28 June 2024

Atmospheric Measurement Techniques Discussions

Appendix B: Data sources

Table B1 presents the different sources used in the current processing and Figure B1 shows the coverage of the sources processed in 2024/01. Figure B2 shows the number of daily processed observations since 2016. Clearly visible is the sudden decrease in number of observation during the COVID19 period.

Table B1. Sources of Mode-S EHS in the processing dd. 2024/01

source	affiliation	main coverage	ATC/local	first data provided
AS-MET	AirSupport, DK	Europe	local receivers	2021-04-15
AU	Austro Control	Austria	ATC radar	2018-09-26
DK	DMI/NAVIAR	Denmark	ATC radar	2017-11-13
ES	AEmet	Spain	ATC radar	2019-06-25
FR	MeteoFrance	France	local receivers	2020-09-08
IL	Israel Meteorological Service	Israel	local receivers	2023-05-01
MUAC	Maastricht Upper Air Control	Benelux	ATC radar	2014-01
NO-FFI	MetNo/FFI	Norway	local receivers	2021-07-03
RO	ROMATSA	Romania	ATC radar	2020-10-01
SE	SMHI	Sweden	local receivers	2021-06-07
SI	SI	Slovenia	ATC radar	2020-09-08
UK	UKMetOffice	United Kingdom	local receivers	2020-02-01

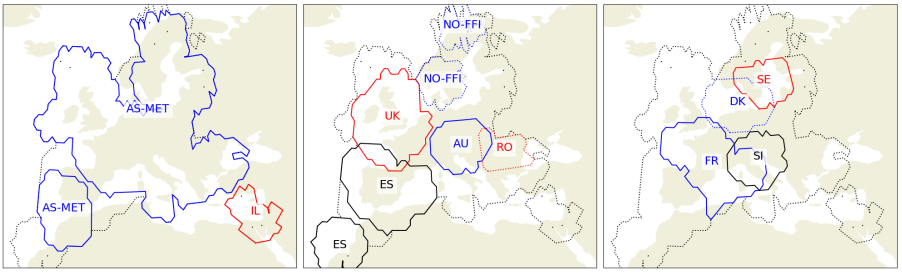

Figure B1. Coverage maps of individual sources: left panel sources AS-MET and IL; middle panel ES, UK, NO-FFI, AU; and right panel : FR, DK, SE and SI.

https://doi.org/10.5194/amt-2024-110
Preprint. Discussion started: 28 June 2024

Atmospheric Measurement Techniques Discussions

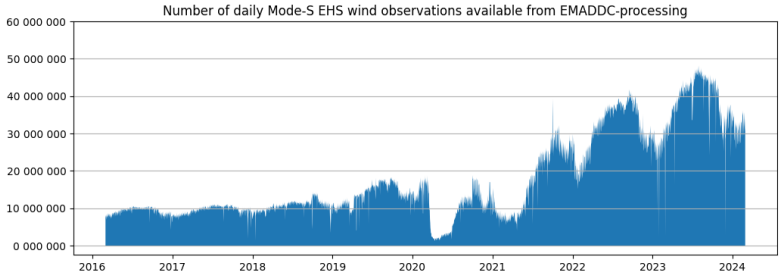

Figure B2. The number of observations per day processed by EMADDC over time.

https://doi.org/10.5194/amt-2024-110
Preprint. Discussion started: 28 June 2024

Atmospheric Measurement Techniques Discussions

Author contributions. Siebren de Haan drafted the manuscript and built the first version of EMADDC and the heading correction algorithm and quality control. Siebren de Haan and Paul de Jong further improved the algorithms and quality control. Paul de Jong and Michal Koutek ported the (research) version to an operational system. Jan Sondij is the EMADDC program manager and the liaison between research and the operational aeronautical meteorological service provision and includes EMADDC funding and stakeholder management. Jan Sondij, Paul de Jong and Michal Koutek provided input for the manuscript draft.

Competing interests. There are no competing interests present.

Acknowledgements. The EMADDC system cannot function without input data in casu Mode-S EHS data. We gratefully acknowledge the delivery of Mode-S EHS data by all our partners for the generation of meteorological information. In particular the provision of Mode-S EHS data by Air Support and the Met Office via a network of local Mode-S/ADS-B receivers. Special thanks go out to Torsten Doernbach from EUROCONTROL MUAC who supported the first and important steps with the MUAC data set and provided continuous support. The EMADDC program is co-financed by the Connecting Europe Facility of the European Union.

https://doi.org/10.5194/amt-2024-110
Preprint. Discussion started: 28 June 2024

References

1207, E.: Commission Implementing Regulation (EU) No 1207/2011 of 22 November 2011 Laying down Requirements for the Performance and the Interoperability of Surveillance for the Single European Sky Text with EEA Relevance, 2011.

Barwell, B. R. and Lorenc, A. C.: A Study of the Impact of Aircraft Wind Observations on a Large-Scale Analysis and Numerical Weather Prediction System, Quarterly Journal of the Royal Meteorological Society, 111, 103–129, 1985.

Benjamin, S. G., Jamison, B. D., Moninger, W. R., Sahm, S. R., Schwartz, B. E., and Schlatter, T. W.: Relative Short-Range Forecast Impact from Aircraft, Profiler, Radiosonde, VAD, GPS-PW, METAR and Mesonet Observations via the RUC Hourly Assimilation Cycle, Monthly Weather Review, 138, 1319–1343, 2010.

Cardinali, C., Isaksen, L., and Andersson, E.: Use and Impact of Automated Aircraft Data in a Global 4DVAR Data Assimilation System, Monthly Weather Review, 131, 1865–1877, 2003.

Chulliat, A.: The US/UK World Magnetic Model for 2015-2020, https://doi.org/10.7289/V5TB14V7, 2015.

de Haan, S.: High-Resolution Wind and Temperature Observations from Aircraft Tracked by Mode-S Air Traffic Control Radar, J. Geophys. Res., 116, D10 111–, https://doi.org/10.1029/2010JD015264, 2011.

de Haan, S.: Assimilation of GNSS ZTD and Radar Radial Velocity for the Benefit of Very-Short-Range Regional Weather Forecasts, Q. J. Roy. Met. Soc., https://doi.org/10.1002/qj.2087, 2013.

de Haan, S., de Jong, P. M. A., and van der Meulen, J.: Characterizing and Correcting the Warm Bias Observed in Aircraft Meteorological Data Relay (AMDAR) Temperature Observations, Atmospheric Measurement Techniques, 15, 811–818, https://doi.org/10.5194/amt-15-811-2022, 2022.

Dube, K.: Emerging from the COVID-19 Pandemic: Aviation Recovery, Challenges and Opportunities, Aerospace, 10, 19, https://doi.org/10.3390/aerospace10010019, 2023.

Ingleby, B., Isaksen, L., and Kral, T.: Evaluation and Impact of Aircraft Humidity Data in ECMWF's NWP System, https://doi.org/10.21957/4e825dtiy, 01/2020 2020.

Ingleby, B., Candy, B., Eyre, J., Haiden, T., Hill, C., Isaksen, L., Kleist, D., Smith, F., Steinle, P., Taylor, S., Tennant, W., and Tingwell, C.: The Impact of COVID-19 on Weather Forecasts: A Balanced View, Geophysical Research Letters, 48, e2020GL090 699, https://doi.org/10.1029/2020GL090699, 2021.

James, E. P., Benjamin, S. G., and Jamison, B. D.: Commercial-Aircraft-Based Observations for NWP: Global Coverage, Data Impacts, and COVID-19, Journal of Applied Meteorology and Climatology, 59, 1809–1825, https://doi.org/10.1175/JAMC-D-20-0010.1, 2020.

Lange, H. and Janjić, T.: Assimilation of Mode-S EHS Aircraft Observations in COSMO-KENDA, Monthly Weather Review, 144, 1697–1711, https://doi.org/10.1175/MWR-D-15-0112.1, 2016.

Li, Z.: Impact of Assimilating Mode-S EHS Winds in the Met Office's High-Resolution NWP Model, Meteorological Applications, 28, e1989, https://doi.org/10.1002/met.1989, 2021.

Maus, S. and Macmillan, S.: 10th Generation International Geomagnetic Reference Field, Eos Trans. AGU, 86, https://doi.org/10.1029/2005EO160006, 2005.

Painting, J. D.: WMO AMDAR Reference Manual, WMO-No.958, WMO, Geneva, 2003.

Petersen, R. A.: On the Impact and Benefits of AMDAR Observations in Operational Forecasting—Part I: A Review of the Impact of Automated Aircraft Wind and Temperature Reports, Bulletin of the American Meteorological Society, 97, 585–602, https://doi.org/10.1175/BAMS-D-14-00055.1, 2016.

https://doi.org/10.5194/amt-2024-110
Preprint. Discussion started: 28 June 2024

Rodi, A. R. and Leon, D. C.: Correction of Static Pressure on a Research Aircraft in Accelerated Flight Using Differential Pressure Measurements, Atmospheric Measurement Techniques, 5, 2569–2579, https://doi.org/10.5194/amt-5-2569-2012, 2012.

Ruijgrok, G. J. J.: Elements of Airplane Performance, Delftse University Pers, 1990.

Strajnar, B.: Validation of Mode-S Meteorological Routine Air Report Aircraft Observations, Journal of Geophysical Research: Atmospheres, 117, https://doi.org/10.1029/2012JD018315, 2012.

Strajnar, B., Žagar, N., and Berre, L.: Impact of New Aircraft Observations Mode-S MRAR in a Mesoscale NWP Model, Journal of Geophysical Research: Atmospheres, 120, 3920–3938, https://doi.org/10.1002/2014JD022654, 2015.

Straus, L.: personal communication, 2020.

Zhu, Y., Derber, J. C., Purser, R. J., Ballish, B. A., and Whiting, J.: Variational Correction of Aircraft Temperature Bias in the NCEP's GSI Analysis System, Monthly Weather Review, 143, 3774–3803, https://doi.org/10.1175/MWR-D-14-00235.1, 2015.